

Silver Selective Electrodes Using Ionophores Functionalized with Thioether–Amide–Amine¹

Nidhi Rani Gupta^a, S. K. Ashok Kumar^b, Susheel K Mittal^c*, Prabhpreet Singh^d, and Subodh Kumar^d

^aDepartment of Chemistry, GSSDGS Khalsa College Patiala, 147001 India

^bDepartment of Chemistry School of Advanced Sciences, VIT University Vellore, 632014 India

^cSchool of Chemistry & Biochemistry, Thapar University Patiala, 147004 India

^dDepartment of Chemistry, Guru Nanak Dev University Amritsar, 143005 India

*e-mail: smittal@thapar.edu

Received April 2, 2015; in final form, July 12, 2016

Abstract—New poly(vinylchloride) (PVC) based liquid membrane sensors are reported containing neutral macrocyclic carrier as potential ionophores for sensing silver ions. Three macrocycles (L₁, L₂ and L₃) possessing two thioether, two amide and one secondary amine unit have been used in new PVC membrane-based sensor. At wide pH range of 4.5 to 8.0, these sensors exhibit linear responses in the concentration range of 1 × 10⁻⁴ to 0.1 M and detection limit 6 × 10⁻⁵ M for L₁ and 1 × 10⁻⁴ M for L₂ and L₃ respectively with pseudo-Nernstian slopes between 43–46 mV/decade for all the three sensors. These sensors have short response time (<15 s) and long life time as these sensors do not show any considerable divergence in their performance over a period of four months. These sensors exhibit good selectivity for Ag⁺ over wide variety of interfering ions like alkali, alkaline earth, transition and some heavy metal ions. These proposed sensors could be used successfully as indicator electrodes in the potentiometric determination of Ag⁺ ions and also to determine anions like Cl⁻, Br⁻, I⁻, S²⁻, SCN⁻ and CN⁻. Potentiometric titrations for halide ions in a mixture using these sensors and new titration method for the determination of detection limits are reported.

Keywords: thioether–amide ionophore, silver ions, liquid membrane electrode, selectivity, potentiometric titrations

DOI: 10.1134/S1061934817020083

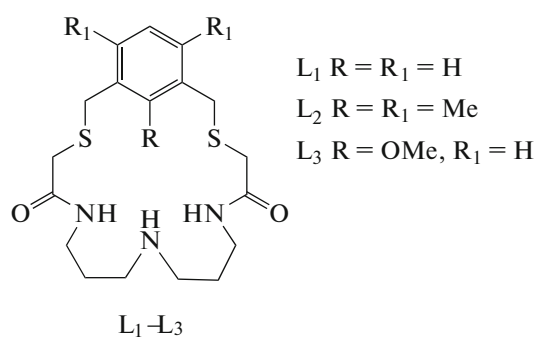
Silver is a metal which is often attracted by people due to its ornamental uses. Besides this property of silver, it has wide use in our daily life. Because of its antibacterial property silver may enter the body through medicinal ointments especially for skin and gums or through handling of silver compounds like in photography. Generally, much less silver will enter the body through the skin than through the lungs or stomach due to use of silver salts and nanoparticles in the disinfection of drinking water [1]. The quick estimation, removal, separation techniques and application of Ag⁺ complexes in industry, biological, medical and daily analysis [2–7] require a fast and efficient method of Ag⁺ determination. There are many well known methods for the determination of silver like atomic absorption spectrometry and inductively coupled plasma in combination with atomic emission or mass spectrometry [8, 9]. While these techniques are quite expensive

and time-consuming, the ion selective sensors are an attracting tool for the same work but in shorter time with good accuracy and precision.

To achieve this target we have designed and synthesized thioether–amide–amine based ionophores (Scheme) which are highly selective for Ag⁺ ions. Preliminary studies show that they forms complexes with Ag⁺ ion in the ratio of 1 : 1. During complexation, two S-atoms and three N-atoms are involved, and the carbonyl oxygen tends to remain away from the complexation [10]. To maintain proper geometry of the molecule with respect to Ag⁺ ion further, derivatives L₂ and L₃ were prepared by placing –CH₃ groups at 2, 4 and 6 positions and a –OCH₃ group at 2 position of *m*-xylene respectively. Central lower part of ionophores favors complexation with silver but serious interferences from other metal ions may be possible. The carbonyl group plays a key role in balancing the molecule during complexation. Depending upon suitable solvent media these molecules as a whole may

¹ The article is published in the original.

undergo complexation. We prepared liquid membrane based ion selective sensors using these neutral carriers (L_1 , L_2 , L_3) to study their analytical aspects for monitoring Ag^+ ions. These sensors could also be applied for the quick and effective monitoring of some anions like Cl^- , Br^- , I^- , S^{2-} , SO_4^{2-} and also SCN^- , CN^- ions which are known carcinogens. All three sensors seem to respond effectively in terms of low cost preparation, quick and easy assays, wide linear range and pH range and no interference by Hg^{2+} – the most interfering metal ion. Some of the reports show serious interference of mercury ions [11] in determination of Ag^+ , but Hg^{2+} is interfering systematically and its presence makes a suitable protecting shield for other metal ion interferences.



Structure of ionophores L_1 , L_2 , L_3 .

EXPERIMENTAL

Reagents. High relative molecular weight poly(vinyl chloride), plasticizers viz., dibutyl phthalate, dioctyl phthalate, bis-2-ethyl sebacate, and *ortho*-nitrophenyloctylether (*o*-NPOE) and all the metal salts were purchased from Sigma-Aldrich, USA. All solvents used in the investigations were of analytical reagent grade. Aqueous salt solutions were prepared by dissolving the appropriate salt in triple distilled deionised water. Potentials were measured with digital potentiometer EQ-602 Equiptronics (accuracy, 0.001 V, India); pH measurements were carried out on an ISFET pH meter (Delta Track, USA). Ionophores (L_1 , L_2 , L_3) were prepared by our research group [10]. Triple distilled deionized water was used throughout the experiments.

Electrode preparation. Membranes of ~0.2 mm thickness were obtained by pouring a solution of 200 mg of the membrane components PVC (33%), ionophore (1–6%), dibutyl phthalate (61–66%), dissolved in 2–3 mL of tetrahydrofuran and evaporated to 1–2 mL at room temperature as per standard procedure [12]. The viscous solution thus obtained was poured on dust-free Pyrex glass plate and the solvent was allowed to evaporate slowly at room temperature.

To obtain membranes with similar characteristics, viscosity of the casting solutions and the rate of solvent evaporation were controlled. The membranes thus obtained were removed from the glass plate and circular pieces of 1.25 cm diameter were cut and mounted on the grounded end of the Pyrex glass tube using adhesive. The membrane was conditioned with $AgNO_3$ solution (0.1 M) for 24 h.

Electromotive force (EMF) measurements. Activity coefficients were calculated according to the Debye–Hückel approximation [13] and EMF values were corrected for liquid-junction potentials with the Henderson equation. All EMF measurements were carried out with the following cell assembly:

SCE | 0.1 M Ag^+ || membrane || Ag^+ test solution | SCE

where SCE – saturated calomel electrode. Membrane potentials were measured with a digital potentiometer (Equip-tronics, India, accuracy ± 0.1 mV) in magnetically stirred solution at room temperature. Silver nitrate solutions for calibrations of the electrodes were obtained by gradual dilution of 0.1 M $AgNO_3$ solution. Salt bridge prepared with agar-agar and potassium nitrate was used in the study.

RESULTS AND DISCUSSION

Characterization of membrane electrode. *Optimization of the membrane composition.* Membrane composition has a significant influence on the sensitivity and selectivity of a sensor [14–18]. Optimum concentration of the ionophores was achieved by changing the ionophore content from 2 to 6% (by weight) with increments of 1% each time (Table 1). In general, the increase in percentage of ionophore increases the slope of calibration curve. However, a diminished response slope of the electrode was observed on further addition of the ionophore most probably due to some in-homogeneity and possible saturation of the membrane [19]. However, the membranes having PVC–plasticizer–ionophore compositions as (33 : 63 : 4, wt %) for L_1 and L_3 and composition (33 : 64 : 3, wt %) for L_2 showed the best responses in terms of both the slope and the measuring range concentration. The nature of the plasticizer affects not only the dielectric constant of membrane phase but also the mobility of ionophore molecules and the state of the ligands [20]. The electrodes based on *o*-NPOE as plasticizer show slopes between 43–46 mV/decade (entries 19 to 21, Table 1).

Effect of pH. The effect of pH on the response behavior of sensors was studied at 0.02 M $AgNO_3$ solution: pH was adjusted with 0.1 M HNO_3 and 0.1 M NaOH solutions as per requirement. It is clear from Fig. 1, that the potential response remains uniform

Table 1. Optimization of membrane ingredients

No	Ionophore	PVC, wt %	Plasticizers, wt %	Ligand, wt %	Slope, mV/decade	Detection limit, M
1	L ₁	33	66	1	7	1.5 × 10 ⁻⁴
2	L ₁	33	65	2	10	1.0 × 10 ⁻⁴
3	L ₁	33	64	3	23	6.3 × 10 ⁻⁵
4	L ₁	33	63 (DBP)	4	35	3.9 × 10 ⁻⁵
5	L ₁	33	62	5	19	1.5 × 10 ⁻⁴
6	L ₁	33	61	6	16	1.2 × 10 ⁻⁴
7	L ₂	33	66	1	8	1.0 × 10 ⁻⁴
8	L ₂	33	65	2	12	1.0 × 10 ⁻⁴
9	L ₂	33	64 (DBP)	3	36	2.5 × 10 ⁻⁴
10	L ₂	33	63	4	24	1.0 × 10 ⁻⁵
11	L ₂	33	62	5	22	1.2 × 10 ⁻⁴
12	L ₂	33	61	6	20	3.9 × 10 ⁻⁴
13	L ₃	33	66	1	25	1.2 × 10 ⁻⁵
14	L ₃	33	65	2	29	1.6 × 10 ⁻⁴
15	L ₃	33	64	3	32	1.2 × 10 ⁻⁴
16	L ₃	33	63 (DBP)	4	40	5.0 × 10 ⁻⁵
17	L ₃	33	62	5	34	1.0 × 10 ⁻⁴
18	L ₃	33	61	6	30	6.3 × 10 ⁻⁵
19	L ₁	33	63 (NPOE)	4	45	5.0 × 10 ⁻⁵
20	L ₂	33	64 (NPOE)	3	43	1.0 × 10 ⁻⁴
21	L ₃	33	64 (NPOE)	4	46	1.0 × 10 ⁻⁴

between the pH range 3.5–8.0, 4.0–8.0 and 4.0–7.5 for L₁, L₂ and L₃, respectively. At pH below this range, the EMF gets altered probably due to protonation of the ionophore and above this pH range due to the formation of AgOH and Ag₂O.

Calibration curve, response time and lifetime of the Ag(I) selective electrode. Calibration curves were drawn for all the three L₁, L₂, L₃ based sensors over a concentration range 10⁻⁶–10⁻¹ M with internal filling solution of Ag⁺ (0.1 M) and showed reproducible slope of 45, 43, and 46 mV/decade respectively. For five repeated experiments, standard deviation of the slope is ±0.5 mV. Representative curves are shown in Fig. 2. The workable concentration range is 1 × 10⁻⁴ to 0.1 M Ag⁺ ions. The limit of detection (5 × 10⁻⁵ M) was calculated according to IUPAC recommendation from the intersection of the two extrapolated linear portions of the curve. Detection limit was also determined by potentiometric titrations of Ag(I) against KI. Potentiometric titrations of Ag⁺ (10⁻², 10⁻³, 10⁻⁴, 10⁻⁵ M) ions against KI (10⁻¹, 10⁻², 10⁻³ and 10⁻⁴ M) were car-

ried out. The same detection limits were obtained by the both methods. The potential break is usually poor in dilute solutions near the end point probably due to weak ionophore–metal ion interaction. The detection limits were also determined by the potentiometric titration curve method (Fig. 3). Due to a sharp change in the slope of the curve at the equivalence point this method was found more reliable and accurate than those obtained by applying the calibration curve method that exhibits irregular curve at lower concentrations [21]. Response time of sensors was <15 s and remained unchanged on measuring potentials either from low to high or high to low concentrations. The lifetime for all three sensors was about four months. During this time the detection limits of the sensor remained almost constant and slope of the sensor varied between ±2 mV of the original value. Sensors were stored in triple distilled water when not in use.

Potentiometric selectivity coefficient. Selectivity coefficient is also called selectivity factor. The selectivity coefficients were determined by fixed interference (FIM) and matched potential (MPM) methods [21,

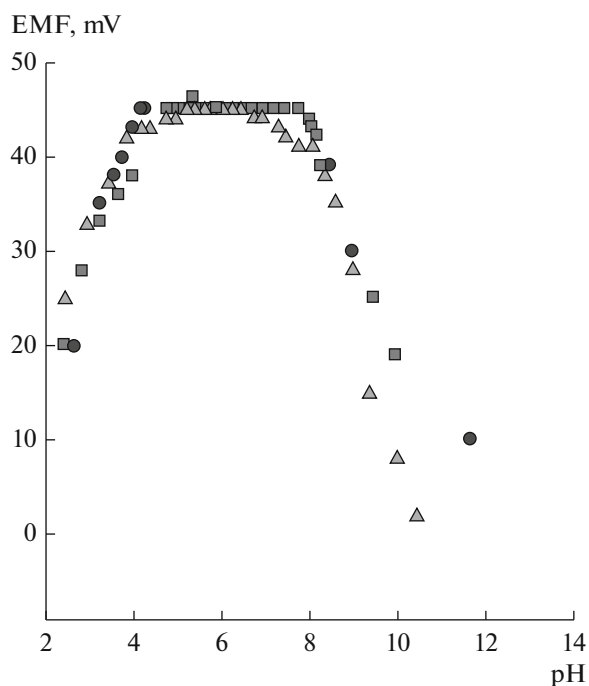


Fig. 1. Effect of pH on the potential response of Ag^+ sensors based on L_1 (■), L_2 (●), and L_3 (▲). Concentration of Ag^+ 1×10^{-2} M.

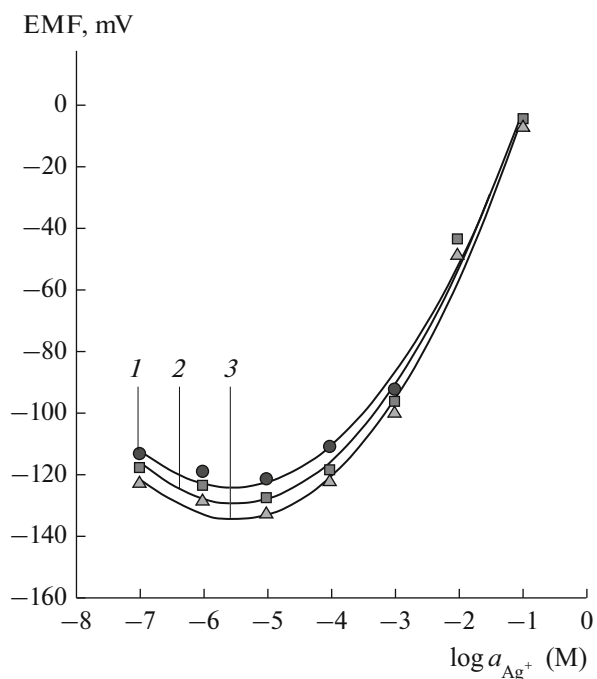


Fig. 2. Calibration curves for Ag^+ ions using L_1 (1), L_2 (2) and L_3 (3) based sensors.

22] and the results are summarized in Table 2. The smaller the value of the selectivity coefficient, the more selective is the electrode for the primary ion in the presence of the interferent. In FIM, a 1×10^{-3} M concentration of interfering ions was used for calculating the selectivity coefficient, whereas in the MPM method, the selectivity coefficients were defined as the ratio of the primary and interfering ion concentrations, which gave the same potential change in the reference solution. To determine the selectivity coefficient by MPM method, one would measure the change in potential upon changing the primary ion concentration. The interfering ion would then be added to an identical reference solution until the same potential change is obtained. The change in potential must be produced in a constant initial background of the primary ion (10^{-4} M) and must be the same in both cases. In this method, there is no need to take the valency of ions into consideration, and therefore, it does not assume that the slopes for both primary and interfering ions are the same or even Nernstian.

It is seen from Table 2 that the sensor based on L_1 gives better values of selectivity coefficients for almost all the interfering ions (by MPM). Further L_2 based sensor shows better selectivity for Ag^+ than L_3 based sensor. The selectivity coefficient values by FIM do not represent a regular trend for the choice of iono-

phore. This may be due to that FIM method is not accurate for the determination of selectivity coefficient, when the charges of ions are different. So, MPM is a better technique to determine selectivity coefficients. Mercury is known to interfere in the determination of Ag^+ ions. In these proposed electrodes the level of interference of Hg^{2+} is the same as that of other bivalent ions like Cd^{2+} , Zn^{2+} and Pb^{2+} . Moreover, the interference of Hg^{2+} is the least for the L_1 electrode in comparison to the two other derivatives due to less hindered molecule with respect to L_2 and L_3 . The selectivity data indicate that values are of the order of 10^{-2} for divalent and trivalent metal ions (except Na^+ and K^+). Therefore, the electrode can be used for the determination of Ag^+ ions in the presence of certain interfering ions.

Effect of electrode response in partially non-aqueous medium. The working nature of the proposed sensors was also studied in partially non-aqueous medium using methanol–water, acetone–water and acetonitrile–water mixtures (Table 3). The sensors based on L_1 , L_2 and L_3 shows satisfactory response to Ag^+ ions in partially non-aqueous medium containing up to 30% (v/v) non-aqueous content. The working range of concentrations (10^{-4} to 0.1 M) is observed in aqueous medium, while the slope has considerably improved values and shows Nernstian behaviour. This is due to

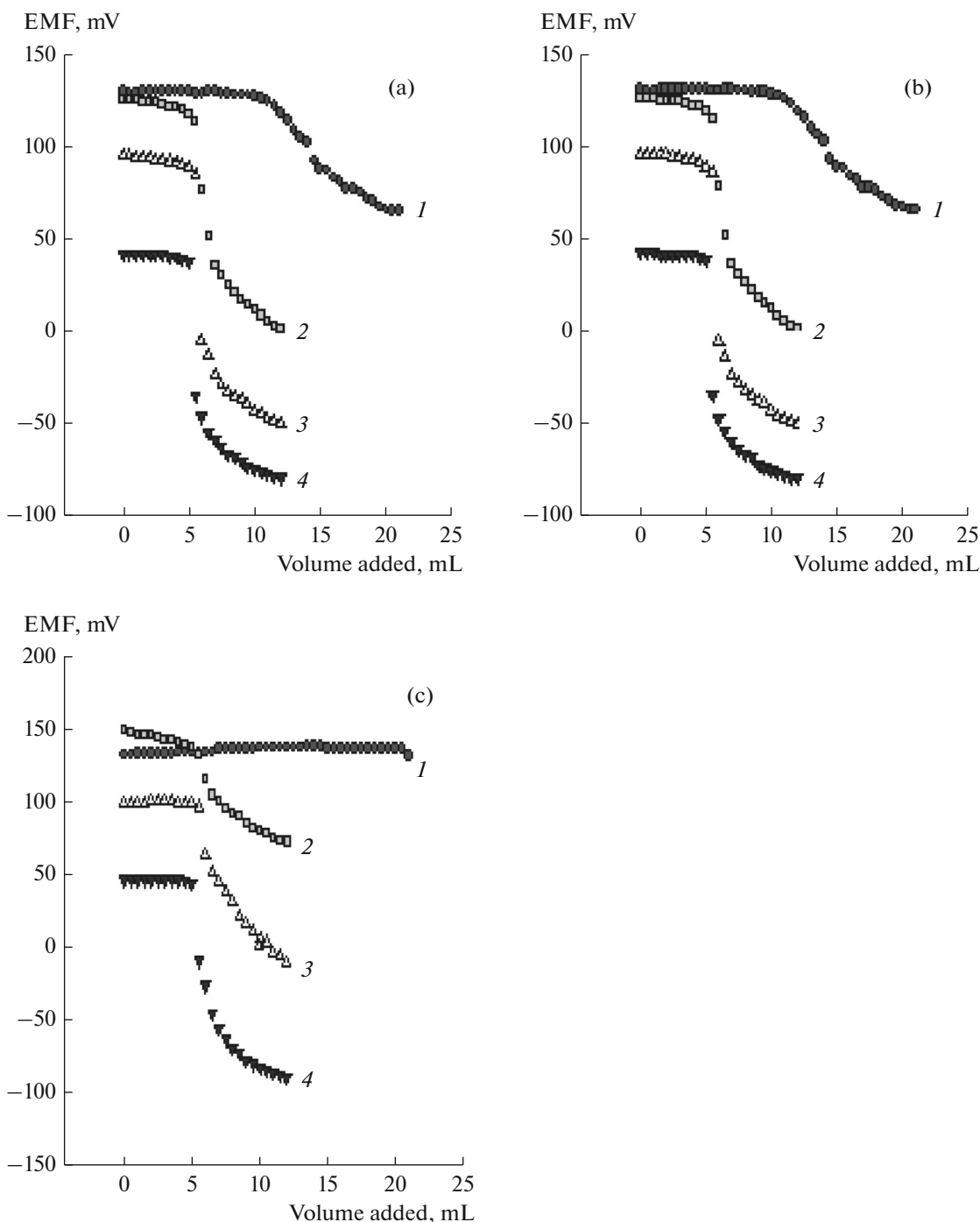


Fig. 3. Determination of detection limits by the potentiometric titration method. Sensors based on L_1 (a), L_2 (b), and L_3 (c): 1— 10^{-5} M Ag^+ vs. 10^{-4} M I^- , 2— 10^{-4} M Ag^+ vs. 10^{-3} M I^- , 3— 10^{-3} M Ag^+ vs. 10^{-2} M I^- , 4— 10^{-2} M Ag^+ vs. 0.1 M I^- .

the changed sheath of solvent around the primary ion Ag^+ . In the aqueous medium H_2O molecules form stable complex with Ag^+ ions, while in partially non-aqueous media, the solvent sheath includes solvent molecules as well, thereby facilitating conduction due to the decrease of dielectric constant of the solvent

mixture while reaching the ionophore. The best results are observed at 20% non-aqueous medium.

Analytical applications. Potentiometric titration. The proposed membrane sensors were found to work well under laboratory conditions. Potentiometric titrations are among the most accurate because the

Table 2. Potentiometric selectivity coefficients ($\log K_{Ag^+, M^{n+}}^{pot}$) by FIM and MPM

Interfering ion	MES-AMD		MXY-AMD		OME-AMD	
	FIM	MPM	FIM	MPM	FIM	MPM
Na ⁺	-1.4	-1.7	-1.2	-1.3	-1.0	-1.1
K ⁺	-1.0	-1.9	-1.1	-1.4	-1.0	-1.2
Mg ²⁺	-2.0	-2.15	-1.8	-2.0	-1.9	-1.7
Ca ²⁺	-1.9	-2.1	-2.4	-1.9	-2.1	-1.8
Sr ²⁺	-2.4	-2.12	-2.1	-2.0	-2.0	-1.9
Co ²⁺	-2.4	-2.16	-2.3	-2.0	-2.0	-1.9
Ni ²⁺	-2.1	-2.17	-2.3	-2.0	-2.1	-1.8
Cu ²⁺	-2.4	-2.18	-2.3	-1.9	-2.2	-1.9
Cd ²⁺	-2.5	-2.2	-2.5	-1.9	-2.0	-2.0
Zn ²⁺	-2.5	-2.19	-2.5	-2.2	-2.0	-2.0
Pb ²⁺	-2.5	-2.17	-2.3	-1.8	-2.3	-1.7
Hg ²⁺	-2.5	-2.2	-2.5	-1.9	-2.5	-1.8
Fe ³⁺	-2.5	-2.3	-2.9	-2.0	-2.8	-2.1

FIM – primary ion concentration varied from 1×10^{-6} to 0.1 M, interfering ion concentration 1×10^{-2} ; MPM – primary ion concentration 1×10^{-4} – 1×10^{-2} M, reference solution 1×10^{-4} M and interfering ion concentration added 1×10^{-2} M.

potential follows the actual change in activity, and therefore the end point will often coincide directly with the equivalence point. A large potential break will occur at the equivalence point. Since we are interested only in the potential change, the correct potential of the indicating electrode need not be known.

The membrane electrodes were immersed in the analyte solution (1×10^{-3} M) I⁻, SCN⁻, CN⁻, etc. and initial EMF was recorded. The titrant (Ag⁺, 1×10^{-2} M) was added in the incremental amounts of 0.5 mL in the titration vessel fitted with a magnetic stirrer system. With each addition a new EMF was observed and recorded. The readings of the EMF val-

ues were plotted as a function of volume of the reagent added from the burette.

Direct and reverse titration of Ag⁺ ions. 50 mL of 1×10^{-3} M Ag⁺ ions solution was titrated against 1×10^{-2} M KI solution (Fig. 4). The potential break was observed at 1 : 1 complex formation between metal ions and I⁻ ions. The same observation was made during reverse titration also.

Potentiometric titrations of binary, ternary and several mixtures of ions. 50 mL of solution containing 1×10^{-3} M Ag⁺ ions in binary, ternary and multi ions mixtures was titrated against 1×10^{-2} M KI solution (Fig. 5). In each titration only one break in EMF cor-

Table 3. Electrode properties in partially non-aqueous medium

Non-aqueous content	Percentage (v/v)	Slope, mV/decade			Detection limit, M		
		L ₁	L ₂	L ₃	L ₁	L ₂	L ₃
Methanol	10 : 90	52	44	50	4×10^{-5}	4×10^{-5}	1×10^{-4}
	20 : 80	54	47	55	5×10^{-5}	5×10^{-5}	1×10^{-4}
	30 : 70	49	46	52	5×10^{-5}	6×10^{-5}	6×10^{-5}
Acetonitrile	10 : 90	55	48	58	1×10^{-4}	8×10^{-5}	5×10^{-5}
	20 : 80	52	55	48	5×10^{-5}	6×10^{-5}	1×10^{-4}
	30 : 70	47	49	44	1×10^{-4}	6×10^{-5}	1×10^{-4}
Acetone	10 : 90	53	53	49	4×10^{-5}	4×10^{-5}	4×10^{-5}
	20 : 80	60	54	54	5×10^{-5}	5×10^{-5}	6×10^{-5}
	30 : 70	52	48	46	6×10^{-5}	8×10^{-5}	1×10^{-4}

responding to AgI complex formation was observed. The titration shows an equivalence point corresponding to the formation of 1 : 1 and 1 : 2 complexes with I⁻ ions. No break in titration was observed corresponding to the complex formation with Hg²⁺ ions. It indicates that the sensors do not respond to Hg²⁺ ions. These results show that mercury is either not interfering or the extent of interference is too small to be measured in silver determination.

It is clearly indicated from the Fig. 5 that 1/3rd (1 equivalent) of the reagent is used up in precipitating the Ag⁺ ions and 2/3rd (2 equivalents) are used up for precipitating the Hg²⁺ ions. However, the extent of Hg²⁺ interference is quite predictable because the inflection in the curve is obtained corresponding to 1 : 3 equivalence. Further, the titrations were done by taking different amounts of Hg²⁺ ions. When it is taken in concentration less than that of Ag⁺ ions, no interference is observed and the titration curve obtained is exactly the same to that as if Hg²⁺ was not present at all. This is due to its high selectivity for silver ions. This is further established from the titration

curve where the EMF remains stable in the pre-equivalence region of the curve and does not change even when the stoichiometric amount of Hg²⁺ is completely precipitated and Ag⁺ starts forming precipitates with iodide ions. During this part of titration, first Hg²⁺ is precipitated because of its lower value $K_{sp}(\text{Hg}_2\text{I}_2) = 10^{-51}$ than Ag⁺ ions $K_{sp}(\text{AgI}) = 10^{-48}$. This indicates that the ionophore is not able to distinguish between Hg²⁺ and Ag⁺ ions when concentrations of Hg²⁺ and Ag⁺ are the same. As the concentration of the interfering ion is decreased (i.e., Hg²⁺ is at lower concentration than Ag⁺) the inflection point of titration is obtained only for the concentration corresponding to silver ions. This shows that the presence of Hg²⁺ ions in the solution is not detected and measured by the sensors. It establishes the great selectivity of Ag⁺ selective electrode in the presence of Hg²⁺ ions. Silver ions were also titrated against iodide ions in the presence of Cu²⁺ and Hg²⁺ ions as ternary mixtures and Cu²⁺, Hg²⁺ and Pb²⁺ as a quaternary mixture. In both the titrations equivalence points were observed corresponding to 3 equivalents of iodide ion. The iodide

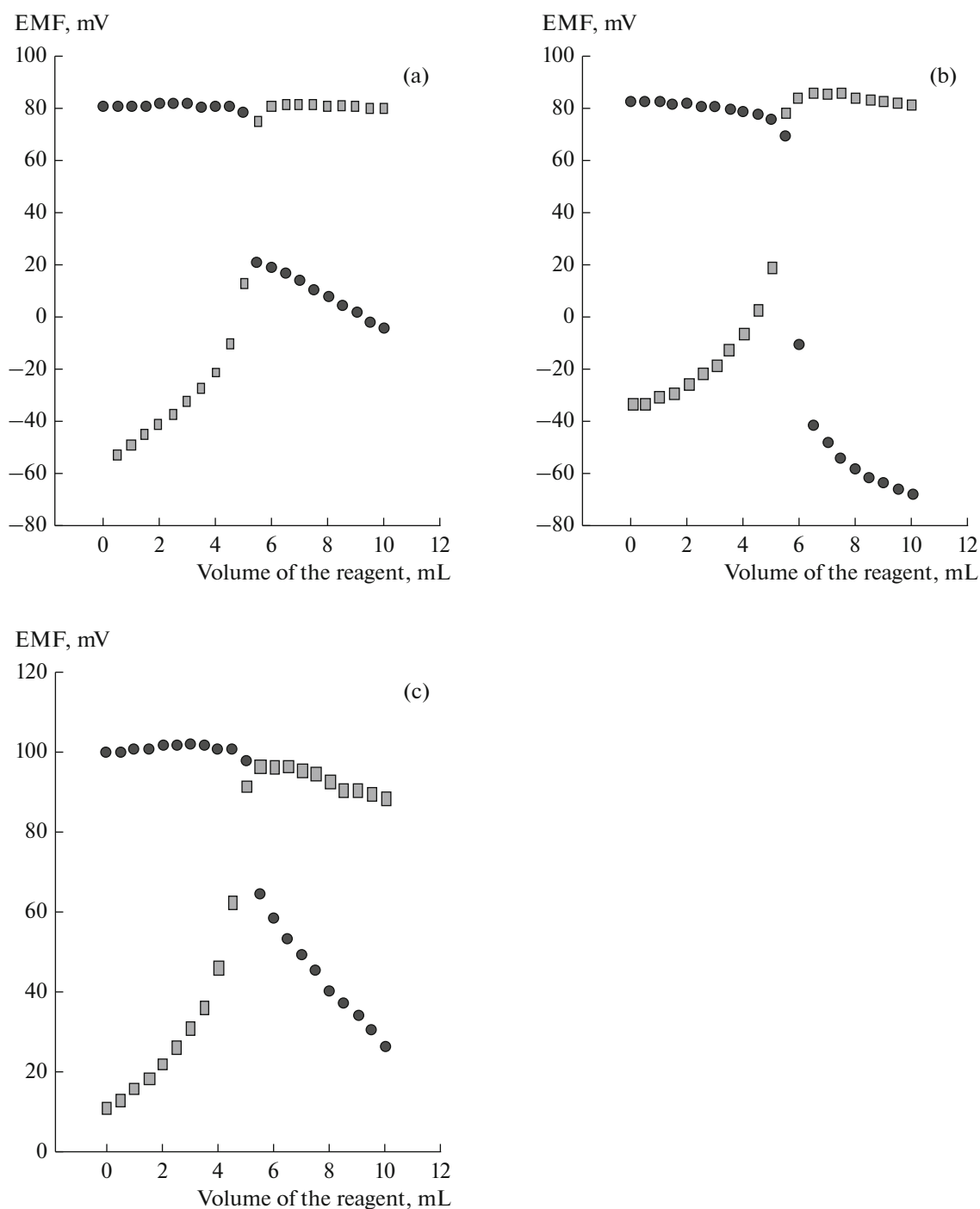


Fig. 4. Direct (●) and reverse (■) potentiometric titrations of Ag^+ ions for L_1 (a), L_2 (b), and L_3 (c) based sensors.

required for Ag^+ is one equivalent and for Hg^{2+} ions is 2 equivalents as reported above in binary titrations. This shows that there is interference only from the

presence of Hg^{2+} and no interference from Cu^{2+} and Pb^{2+} ions. So the electrode behaves in a highly selective manner for Ag^+ ion determination.

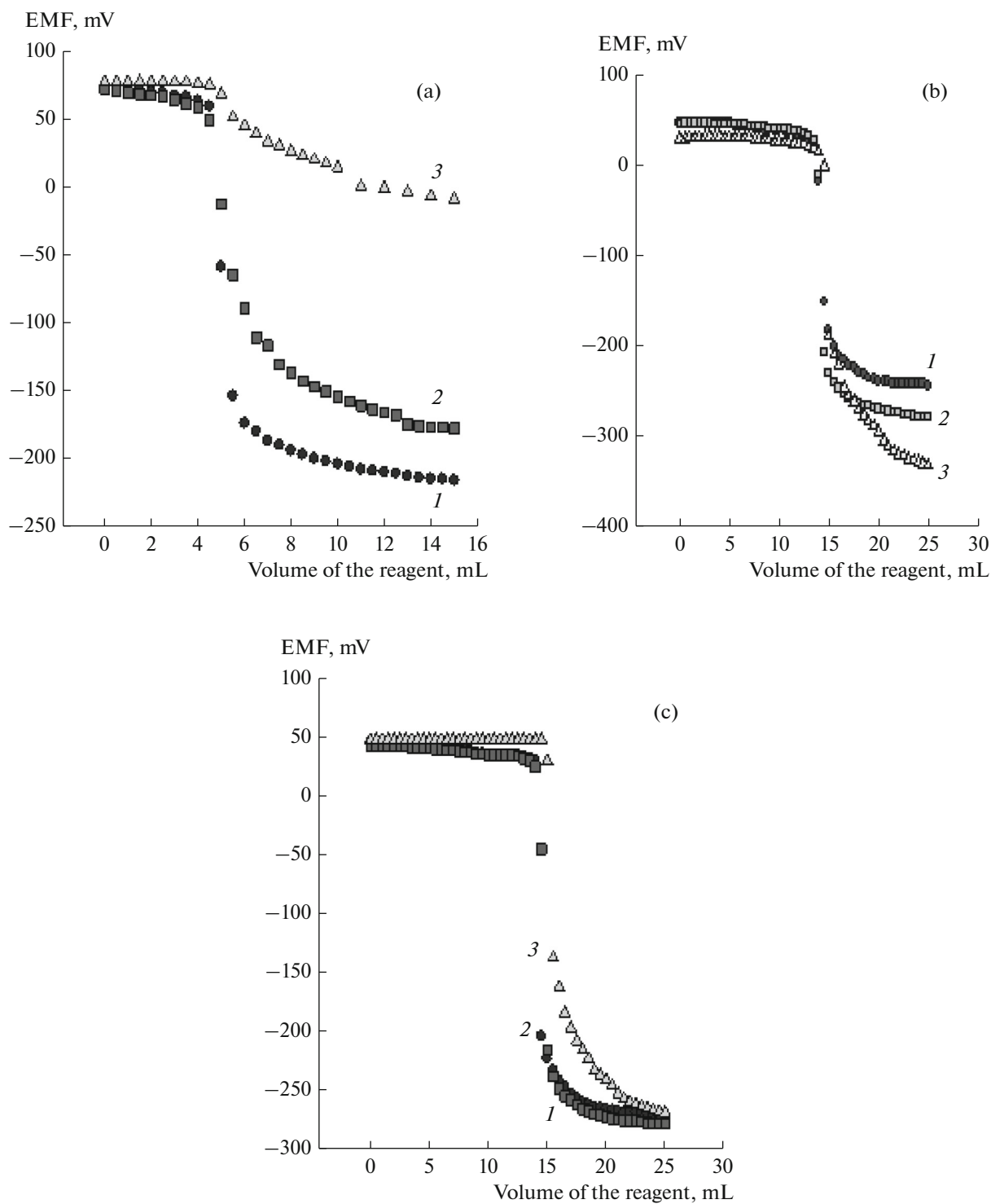


Fig. 5. Determination of silver content in the presence of interfering metal ions (Cu^{2+} , Hg^{2+} and Pb^{2+}) in binary, ternary and quaternary titrations, respectively. Sensors based on L_1 (1), L_2 (2) and L_3 (3); (a) 50 mL of $1 \times 10^{-3} \text{ M}$ (Ag^+ and Cu^{2+}) vs. $1 \times 10^{-2} \text{ M}$ KI, (b) 50 mL of $1 \times 10^{-3} \text{ M}$ (Ag^+ , Cu^{2+} and Hg^{2+}) vs. $1 \times 10^{-2} \text{ M}$ KI, (c) (Ag^+ + Cu^{2+} + Hg^{2+} + Pb^{2+}) vs. KI.

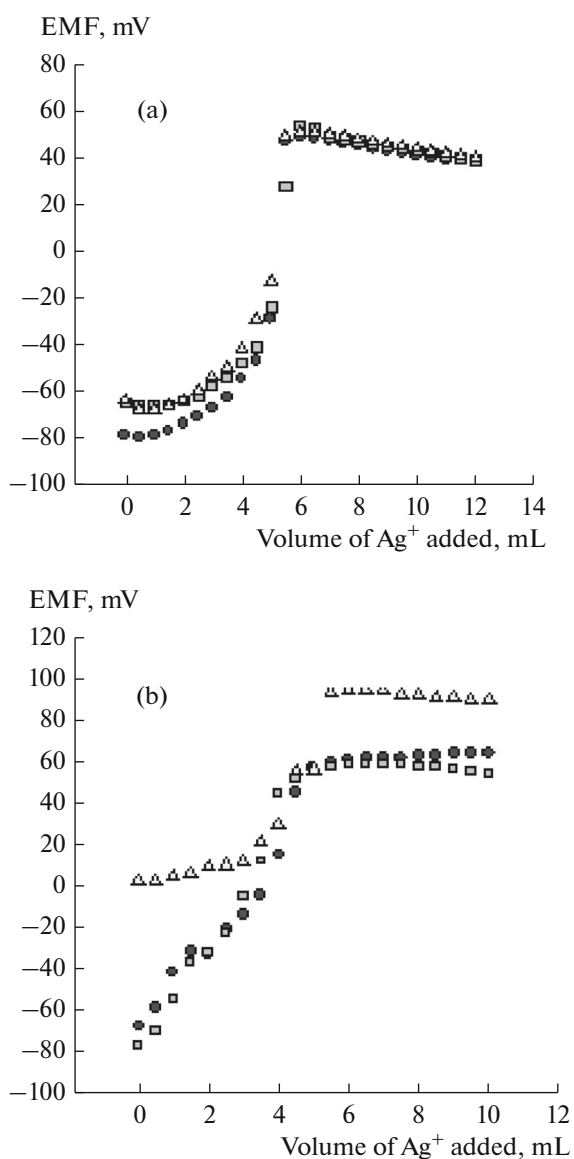


Fig. 6. Potentiometric titration of SCN⁻ (a) and CN⁻ (b) against Ag⁺ using L₁ (●), L₂ (■) and L₃ (Δ) ionophore based sensors.

Low level potentiometric determinations of CN⁻ and SCN⁻ ions. The proposed sensors were also used as probes for the determination of carcinogenic anions like SCN⁻ and CN⁻ in water samples, since Ag⁺ shows a great affinity to these ions (Fig. 6). The break in slopes corresponded to 1 : 1 complex formation. All the three ionophores L₁, L₂, L₃ show similar behavior during the potentiometric titrations. Performance of the electrode has been compared and summarized in Table 3 with reported ones [23–28] in terms of sensitivity, selectivity, life time and use in the determination of anions.

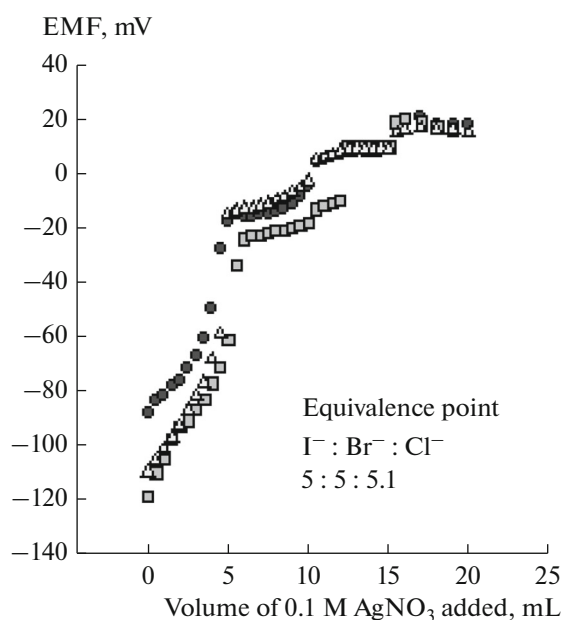


Fig. 7. Determination of halide mixtures present in sample solution using L₁ (●), L₂ (■) and L₃ (Δ) based sensors (50 mL of 10⁻² M X⁻ vs. 0.1 M Ag⁺).

Potentiometric determinations of Cl⁻, Br⁻ and I⁻ contents in a mixture. Figure 7 shows three breaks in the curve corresponding to precipitation of Ag⁺ with each ion in the ratio 1 : 1; the first break is for I⁻, the second and third breaks in curve are for Br⁻ and Cl⁻; respectively. This trend can be explained on the basis of solubility product. The K_{sp} values change in the order I⁻ < Br⁻ < Cl⁻.

On the basis of the performance of all the sensors described in this work, L₁, L₂ and L₃ can be used as electro-active ionophores to prepare sensors for Ag⁺ ions with excellent characteristics like linear response, sensitivity and selectivity for a number of common interfering ions shown in Table 4. The applications of silver sensors for anion estimations are extremely good. This may be due to good complexing ability of the ligand for Ag⁺ ions and anion. The membrane sensors were used as indicator electrodes in the potentiometric titrations of a mixture of halides (Cl⁻, Br⁻ and I⁻).

ACKNOWLEDGMENTS

SKM is thankful to Thapar University, Patiala, for the research work. NRG acknowledges Department of Science and Technology (India) for the assistance-

Table 4. Comparison of performance of proposed sensors with reported

Measuring range, M	Slope mV/decade	pH range	Lifetime, months	Method of detection limit determination	$\log K_{Ag^+,B}^{pot}$	Used for anion determination	Reference
10^{-5} – 10^{-1}	Nernstian	1–6	6	From calibration curve	Sufficiently selective	NR	[11]
10^{-6} – 10^{-1}	Nernstian	2.5–6.5	NM	From calibration curve	Highly selective	NR	[23]
10^{-2} – 10^{-6}	Near Nernstian	2.5–7	NM	From calibration curve	Sufficiently selective	NR	[24]
10^{-4} – 10^{-1}	Nernstian	–	NM	From calibration curve	Sufficiently selective	NR	[25]
10^{-6} – 10^{-1}	Nernstian	2.5–8.5	3	From calibration curve	Highly selective	NR	[26]
10^{-5} – 10^{-1}	Nernstian	1–10	NM	From calibration curve	Sufficiently selective	NR	[27]
10^{-6} – 10^{-2}	Near Nernstian	2.8–12	NM	From calibration curve	Sufficiently selective	NR	[28]
10^{-5} – 10^{-1}	Pseudo-Nernstian	4.5–8.0	4–5	Calibration curve and potentiometric titration method	Highly selective	Cl^- , Br^- , I^- , CN^- , SCN^-	Present work

Notations: NM—not mentioned, NR—not reported.

ship under DISHA scheme [DST/DISHA/SoRF-PM/024/2013]. SK thanks UGC for center for advanced studies to chemistry department, GNDU, Amritsar and DST for financial assistance. Ashok Kumar SK is thankful to VIT University, Vellore for the support.

REFERENCES

1. Farhang, M., Moradi, M., and Faridbod, F., *Anal. Bioanal. Electrochem.*, 2013, vol. 5, p. 352.
2. Yu, C.W., Zhang, J., Ding, M.Y., and Chen, L.X., *Anal. Methods*, 2012, vol. 4, p. 342.
3. Zhang, J., Yu, C.W., Lu, G., Fu, Q.Y., Li, N., and Ji, Y.X., *New J. Chem.*, 2012, vol. 36, p. 819.
4. Wu, S.J., Zhang, J., Lu, W.J., Zhang, H.Y., Shen, D.Z., and Pan, D.W., *Int. J. Electrochem. Sci.*, 2012, vol. 7, p. 3567.
5. Zhang, J., Ding, J.W., Yin, T.J., Hu, X.F., Yu, S.Y., and Qin, W., *Talanta*, 2010, vol. 81, p. 1056.
6. Blaser, S.A., Scheringer, M., Macleod, M., and Hungerbühler, K., *Sci. Total Environ.*, 2008, vol. 390, p. 396.
7. Mittal, S.K., Ashok Kumar, S.K., Gupta, N.R., Ocak, M., and Ocak, U., *Ind. J. Chem.*, 2008, vol. 47A, p. 1676.
8. Kenneth, H., *Official Methods of Analysis of the Association of Official Analytical Chemists*, Arlington, VA: AOAC, 1990.
9. EPA Method 200.7: Inductively coupled plasma atomic emission spectrometric method for trace element analysis of water and wastes and EPA Method 200.8: Determination of trace elements in waters and wastes by inductively coupled plasma—mass spectrometry, *Methods for Determination of Metals in Environmental Samples, Supplement I*, Environmental Protection Agency, EPA-600/R-94-111, May, 1994.
10. Singh, P. and Kumar, S., *J. Incl. Phenom. Macrocycl. Chem.*, 2007, vol. 59, p. 155.
11. Chen, L., He, X., Zhao, B., and Liu, Y., *Anal. Chim. Acta*, 2000, vol. 417, p. 51.
12. Craggs, A., Moody, G.J., and Thomas, J.D.R., *J. Chem. Educ.*, 1974, vol. 51, p. 541.
13. Kielland, J., *J. Am. Chem. Soc.*, 1937, vol. 59, p. 1675.
14. Mittal, S.K., Kumar, P., Ashok Kumar, S.K., and Lindoy, L.F., *Int. J. Electrochem. Sci.*, 2010, vol. 5, p. 1984.
15. Gupta, N.R., Mittal, S.K., Kumar, S., and Ashok Kumar, S.K., *Mater. Sci. Eng., C*, 2008, vol. 28, p. 1025.
16. Gupta, N.R., Mittal, S., and Kumar, S.S., *Adv. Sci. Eng. Med.*, 2013, vol. 5, p. 1.
17. Mittal, S.K., Ashok Kumar, S.K., Gupta, N., Kaur, S., and Kumar, S., *Anal. Chim. Acta*, 2007, vol. 585, p. 161.
18. Buhlmann, P., Pretsch, E., and Baker, E., *Chem. Rev.*, 1998, vol. 98, p. 1593.
19. Ammann, D., Pretsch, E., Simon, W., Lindner, E., Bezegh, A., and Pungor, E., *Anal. Chim. Acta*, 1985, vol. 171, p. 119.
20. Morf, W.E., *The Principles of Ion-Selective Electrodes and Membrane Transport*, New York: Elsevier, 1981.
21. Buck, R.P. and Lindner, E., *Pure Appl. Chem.*, 1994, vol. 66, p. 2527.
22. Umezawa, Y., Umezawa, K., and Sato, H., *Pure Appl. Chem.*, 1995, vol. 67, p. 507.
23. Amini, M.K., Ghaedi, M., Rafia, A., Baltork, I.M., and Niknamb, K., *Sens. Actuators, B*, 2003, vol. 96, p. 669.
24. Kimura, K., Yajima, S., Tatsumi, K., Yokoyama, M., and Oue, M., *Anal. Chem.*, 2000, vol. 72, p. 5290.
25. Lim, S.M., Chung, H.J., Paeng, K.J., Lee, C.H., Choi, H.N., and Lee, W.Y., *Anal. Chim. Acta*, 2008, vol. 453, p. 81.
26. Mahajan, R.K., Kaur, I., and Kumar, M., *Sens. Actuators, B*, 2003, vol. 91, p. 26.
27. Mahajan, R.K., Kaur, I., Sharma, V., and Kumar, M., *Sensors*, 2002, vol. 2, p. 417.
28. Mashhadizadeh, M.H., Mostafavi, A., Abadi, H.A., and Sheikhshoai, I., *Sens. Actuators, B*, 2006, vol. 113, p. 930.